



Ghost diffraction: A spatial statistical approach

Manisha^a, Vipin Tiwari^b, Nandan S. Bisht^{b,c}, Bhargab Das^d, Rakesh Kumar Singh^{a,*}

^a Laboratory of Information Photonics and Optical Metrology, Department of Physics, Indian Institute of Technology (Banaras Hindu University), Varanasi, 221005, Uttar Pradesh, India

^b Applied Optics & Spectroscopy Laboratory, Department of Physics, Kumaun University, SSJ Campus Almora 263601, Uttarakhand, India

^c Department of Physics, Soban Singh Jeena University, Almora 263601, Uttarakhand, India

^d Micro-Nano Optics Center, CSIR-Central Scientific Instruments Organization, Sector 30-C, Chandigarh 160030, India

ARTICLE INFO

Keywords:

Imaging
Speckle
Scattering media
Phase retrieval

ABSTRACT

We report a new method to reconstruct a two-dimensional object in Ghost diffraction scheme using a spatial statistical optics approach. This is implemented by using a static diffuser rather than a pseudo thermal light source generated with a rotating diffuser as used in conventional ghost imaging systems. The experimental implementation makes use of spatial ergodicity and spatial stationarity for spatially distributed random fields by following an analogy between time average and space average. The ensemble average is replaced by space average under the condition of spatial stationarity and ergodicity. A strategy to realize the Ghost diffraction scheme through spatial intensity correlation with a phase retrieval algorithm permits reconstruction of the transparency.

1. Introduction

Image recovery elicited from the correlation of a stochastic light has been the subject of significant research interest in the classical and quantum domains [1–3]. Over the past few years, a plethora of attention has been shown to recover the image using the intensity correlation between two light fields, and techniques such as ghost diffraction (GD) and ghost imaging (GI) have emerged [4–8]. Compared to conventional imaging techniques, the GD & GI uses a non-spatially resolved bucket detector to collect light originating from a transparency either in reflection or transmission geometry. In these techniques, one light field interacts with the transparency and is detected by a bucket detector. The second light field which does not interact with the object; directly propagates to the spatially resolved detector having an array of pixels. A spatial structure and diffraction pattern of the transparency image can be retrieved by correlating the information measured by the bucket with the information recorded by the array detector in the second arm which never interacts with the transparency. The GD and GI were initially demonstrated with the entangled photons generated in spontaneous parametric down-conversion [9,10]. It was demonstrated later that quantum entangled sources are not necessary and realizations of GD and GI are also possible with the classical correlated light [11] as well as thermal light [12,13]. Since then, significant attention has been attributed to these techniques with classical light for applications in remote sensing [14], biomedical optics [15], microscopy [16], temporal imaging [17], averaged speckle patterns [18] etc. Another important trend in the GD and GI make use of digital insertion of the random

phase masks in coherent light to realize computational imaging [19–21].

However, major interests in the GD and GI are limited to recovery of only the modulus square of the Fourier spectrum [13,22,23], without a phase recovery except for some investigations. A modified Young's interferometer was employed to measure the field correlation in the GD and to recover the phase information [24]. A few ghost schemes have also been developed with specific attention to phase recovery [25–27]. Recently, phase recovery in the GD has been demonstrated using the interference of coherent waves using the spatially fluctuating field. This technique uses a combination of Mach–Zehnder interferometers, i.e., inner and outer interferometer assembly [28]. Experimental implementations on the GD & GI usually employ rotating ground glass (RGG) to mimic a pseudo thermal light source. Such experimental implementation uses temporal averaging as a substitute for ensemble averaging on the premise of temporal stationarity and temporal ergodicity.

On the other hand, a spatial statistical regime is equally important and needs attention in a situation where temporal averaging is not possible. For instance, spatial statistics of the randomly scattered coherent field, such as laser speckle, provide useful statistical information. Moreover, it permits the replacement of the ensemble average by the spatial average under consideration of spatial stationarity and spatial ergodicity [29]. In spite of its practical importance and common occurrence, spatial fluctuations of laser speckles appear to have not attracted attention in the GD & GI except a recent investigation [28].

* Corresponding author.

E-mail address: krakseshsingh.phy@iitbhu.ac.in (R.K. Singh).

To fill this gap and explore the use of spatial ergodicity, we propose and demonstrate the GD scheme with a static ground glass (SGG) rather than RGG. The idea is to examine the reconstruction of a transparency image using basic principle of the GD with the spatial statistical optics approach. Moreover, a phase retrieval algorithm is combined with the results of the GD to retrieve the transmission function of a planar object. This strategy helps to recover the transparency information using spatial intensity correlation between the random fields from a single pixel of a detector and array of pixels without object in the GD scheme. Here, single pixel in our scheme refers use of only one pixel intensity of the random light coming from the object arm. This single pixel of a detector at the observation plane is a replacement of the single pixel detector used in the GD. Experimental tests of the proposed scheme are carried out, and experimental results are compared with simulation results. A good agreement between the experiment and simulation supports the use of a new reconstruction approach in the correlation based imaging, and spatial statistical optics approach for Ghost Diffraction studies. Moreover, a quantitative analysis of retrieved results is provided by utilizing the visibility and reconstruction efficiency parameters. The detailed theoretical explanation, method, and corresponding experimental and simulation results are presented below.

2. Methodology

A comparison of the GD setup with RGG, and our experimental geometry of the proposed technique with the SGG is shown in Fig. 1. Usually, the RGG generates temporally fluctuating speckle patterns for realization of the ensemble averaging as shown in Fig. 1(a). Here, we present realization of the ensemble average by the spatial averaging [29], and two replicas of the speckle pattern are utilized. Therefore, RGG is replaced by a static ground glass (SGG) as shown in Fig. 1(b). Consider two identical copies of the light field distribution at a source plane, say $z = 0$. Let $E(r)$ denote the optical field at a particular instant of time, i.e., a single realization of the RGG. A beam splitter (BS) is used to create two copies of the optical field. Furthermore, at the plane $z = 0$, one of the two copies illuminates the transparency $\tau(r)$ and propagates to the observation plane. Consider the propagation of a monochromatic light field from source plane to observation plane at a distance $z = d$ in the Ghost diffraction (GD) scheme. The instantaneous light fields reaching at the observation plane are represented as

$$E_1(u) = \int \tau(r) E_1(r) G(u-r) dr \quad (1)$$

$$E_2(u) = \int E_2(r) G(u-r) dr \quad (2)$$

where r and u are the spatial coordinates at source plane and observation plane respectively. $E_1(u)$ is the light field at detector plane with the transparency $\tau(u)$ and $E_2(u)$ is light field reaching at the observation plane without carrying transparency as desired in the GD. The term $G(u, r)$ denotes the propagation kernel which is represented as,

$$G(u, r) = \frac{\exp(ikz)}{i\lambda z} \exp\left(ik \frac{|u|^2 + |r|^2 - 2ur}{2z}\right) \quad (3)$$

where $k = \frac{2\pi}{\lambda}$ and λ are the wave number and wavelength of light respectively. Propagation distance is denoted by z .

Therefore, the light field at the observation plane is given as

$$E_1(u) = \frac{\exp(ikz)}{i\lambda z} \exp\left(\frac{|u|^2}{2z}\right) \iint \exp\left(ik \frac{|r_1|^2 - 2ur_1}{2z}\right) E_1(r_1) \tau(r_1) dr_1 \quad (4)$$

$$E_2(u) = \frac{\exp(ikz)}{i\lambda z} \exp\left(\frac{|u|^2}{2z}\right) \iint \exp\left(ik \frac{|r_2|^2 - 2ur_2}{2z}\right) E_2(r_2) dr_2 \quad (5)$$

The transparency information is encoded into the spatial correlation functions of the intensities $\langle I_1(u_1) I_2(u_2) \rangle$. The intensities in two different arms of the GD scheme are represented as,

$$I_1(u_1) = E_1^*(u_1) E_1(u_1) \quad (6)$$

$$I_2(u_2) = E_2^*(u_2) E_2(u_2) \quad (7)$$

A correlation of intensity fluctuation of these two spatially fluctuating light fields is represented as,

$$g^2(u_1, u_2) = \langle \Delta I_1(u_1) \Delta I_2(u_2) \rangle = \langle I_1(u_1) I_2(u_2) \rangle - \langle I_1(u_1) \rangle \langle I_2(u_2) \rangle \quad (8)$$

where, $\Delta I_p(u) = I_p(u) - \langle I_p(u) \rangle$ is the fluctuation of intensity at a location u over its mean value, and $\langle \rangle$ represents the ensemble average.

Using Eq. (6), (7) and substituting Eq. (4) & (5) into Eq. (8) results into cancellation of the phase curvature outside the integral $\frac{\exp(ikz)}{i\lambda z} \exp\left(\frac{|u|^2}{2z}\right)$ and this helps to get the spatial ergodicity and spatial stationarity at the observation plane. Moreover, correlation of intensity fluctuations can be expressed as modulus square of the two-point field correlation as

$$g^2(u_1, u_2) = \left| \langle E_1^*(u) E_2(u + \Delta u) \rangle \right|^2 \quad (9)$$

For further calculations, let us consider a change of variables, $u_2 = u + \Delta u$ and $u_1 = u$. The field correlation can be extracted by applying the spatial averaging as a replacement of the ensemble averaging,

$$\begin{aligned} \langle E_1^*(u) E_2(u + \Delta u) \rangle &= \iiint E_1^*(r_1) \tau(r_1) E_2(r_2) \\ &\exp\left(\frac{-ik(|r_1|^2 - |r_2|^2)}{2z}\right) \exp\left(\frac{-ik((u + \Delta u) \cdot r_2 - u \cdot r_1)}{z}\right) dr_1 dr_2 du \\ &= \iint \frac{E_1^*(r_1) \tau(r_1) E_2(r_2) \exp\left(\frac{-ik(|r_1|^2 - |r_2|^2)}{2z}\right)}{\exp\left(\frac{-ik(\Delta u \cdot r_2)}{z}\right)} \left[\int \exp\left(\frac{-ik(r_2 - r_1) \cdot u}{z}\right) du \right] dr_1 dr_2 \end{aligned} \quad (10)$$

Here, we employ the following equation using space averaging under the condition of spatial stationarity and ergodicity and follows the same analogy as used in temporal averaging. Therefore, ensemble average is supplanted by space averaging instead of time averaging.

$$\int \exp\left(\frac{-ik((r_2 - r_1) \cdot u)}{z}\right) du = \delta(r_2 - r_1) \quad (11)$$

Therefore, Eq. (10) takes the form of,

$$\langle E_1^*(u) E_2(u + \Delta u) \rangle = \int I(r) \tau(r) \exp\left(\frac{-i2\pi \Delta u \cdot r}{\lambda z}\right) dr \quad (12)$$

$$\langle E_1^*(u) E_2(u + \Delta u) \rangle \propto \int \tau(r) \exp\left(\frac{-i2\pi \Delta u \cdot r}{\lambda z}\right) dr \quad (13)$$

where, we have considered $r_2 = r_1 = r$ and Eq. (13) is considered under assumption of uniform illumination intensity at the source, i.e. $I(r) = 1$.

Utilizing the spatial stationarity at the observation plane and considering $u_2 = u + \Delta u$ and $u_1 = u$, the correlation of the intensity fluctuations can now be represented as

$$g^2(\Delta u) = |F(\Delta u)|^2 \quad (14)$$

where $|F(\Delta u)| = \left| \tau\left(k \frac{\Delta u}{d}\right) \right|$ is the amplitude of Fourier transform of transparency $\tau(r)$. Eq. (14) states that the correlation between intensity fluctuations reconstructs the amplitude of the Fourier spectrum of the transparency. Moreover, Fourier spectrum depends only on the difference between two coordinates, i.e., $(u_2 - u_1)$. The spatial distribution of the Fourier spectrum is obtained by spatially varying the detection point in the reference arm and keeping the detection position of the transparency arm at $u_1 = 0$. However, the phase distribution of the Fourier spectrum is lost in Eq. (14) and this obstructs recovery of the transparency $\tau(r)$. To overcome this issue, we make use of a

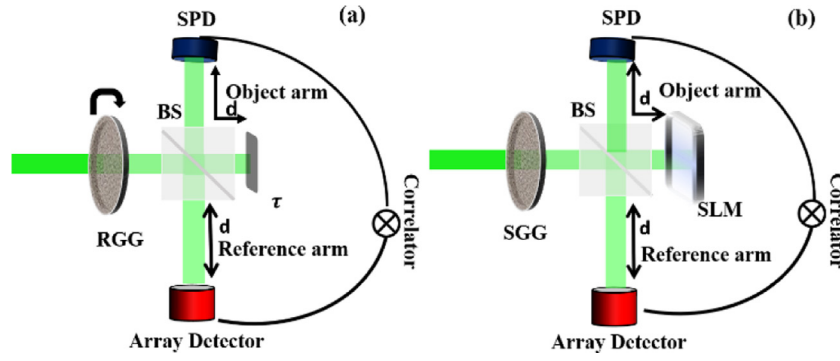


Fig. 1. Conceptual representations of a GD scheme with RGG and our proposed GD scheme (a) ghost diffraction scheme with RGG: rotating ground glass, SPD: Single Pixel Detector, transparency- $\tau(r)$, reflective type. (b) Proposed ghost diffraction scheme with SGG: Static Ground Glass, BS: Beam Splitter.

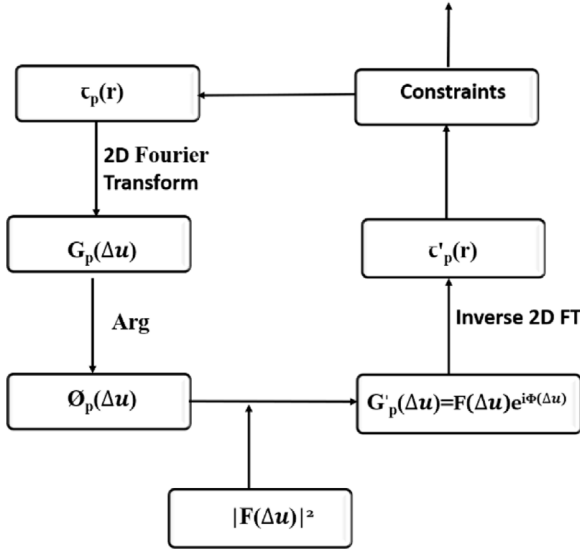


Fig. 2. Block diagram for the phase retrieval algorithm.

phase retrieval algorithm; Fienup type algorithm [30–32] by using few constraints. This helps to resolve the phase loss problem in the intensity correlation measurement. The correlation of the intensity fluctuations obtained in Eq. (14) is subjected to the phase retrieval algorithm with the constraint that the $\tau(r)$ is real and positive. Additionally, we also applied a loose support constraint (the support is the set of points over which the object function is nonzero). Prior to using the phase retrieval approach, the noisy regions of the intensity correlation function were removed from the observed far field using a 2D Tucky window. A hybrid input–output (HIO) algorithm with a fixed β value is used to implement the phase retrieval algorithm, where β is the feedback parameter that controls the convergence properties of the HIO algorithm. Moreover, the residual noise from the retrieved image is reduced using an error-reduction method. [32]. A flow chart for the understanding of implementation of the phase retrieval algorithm is given in Fig. 2.

The algorithm starts with an initial guess of transparency $\tau(r)$, which is fed to the process as mentioned in Fig. 2. Amplitude of the Fourier spectrum obtained in Eq. (14) is fed to the algorithm and process goes on for p th iterations. By applying the constraints to the transparency that it should be real and non-negative, the output of the p th iteration, $\tau'_p(r)$ is used as an input for the next $(p + 1)$ th iteration. Now few iterations of hybrid input output algorithm (HIO) are implemented as following.

$$\tau_{p+1}(r) = \begin{cases} \tau'_p(r) & \text{for } r \notin S \\ \tau_p(r) - \beta\tau'_p(r) & \text{for } r \in S \end{cases} \quad (15)$$

Further the output of HIO algorithm is applied to an error reduction algorithm which is described as below.

$$\tau_{p+1}(r) = \begin{cases} \tau'_p(r) & \text{for } r \notin S \\ 0 & \text{for } r \in S \end{cases} \quad (16)$$

S is the set of all points on $\tau'_p(r)$ that does not follow the constraints. Several iterations were performed and different values of β were used for the faithful reconstruction with a good convergence. Thus, with the help of the mentioned algorithm, the transparency function is retrieved from the amplitude variation of the Fourier spectrum of transparency obtained in Eq. (14).

To demonstrate the proposed technique, we simulate the experimental scheme as shown in Fig. 1(b) and confirm it experimentally.

3. Experiment

Experimental setup of the proposed technique is shown in Fig. 3. A monochromatic laser beam (532 nm) is spatially filtered and collimated with the help of a collimating lens (L). This collimated beam of diameter 4.8 mm illuminates a SGG, and the randomly scattered field splits into two parts by a BS. The light transmitted from the BS is dumped. The reflected beam goes to a spatial light modulator TNLC-SLM (LC-R720 model manufactured by HOLOEYE) to insert transparency $\tau(r)$ into the light. The beam reflected from SLM goes back to the BS; and travels to a detector where we use only a single pixel of the detector for a selected patch of the intensity. A polarizer (P) with axis horizontal, is placed right before the detector to make the uniform polarization in the recorded speckle pattern. The detection plane is located at a distance $d = 150$ mm from the SLM. In the second case, the SLM is switched off and the speckle pattern reflected by the SLM travels back to the detector plane and is recorded by an array of pixels of the charged coupled device (CCD). The CCD camera has a pixel resolution of 2200×2752 and pixel size $4.54 \mu\text{m}$ (Procilica, GT-2750).

Detailed procedure to evaluate the spatial intensity correlation in the GD scheme with the spatial statistical optics is explained in Fig. 4. A random field reflected by the transparency is recorded by detector and only a single pixel data of the intensity patch is used as shown in Fig. 4(a). On the other hand, the second random field is recorded by array of pixels with the SLM off condition, i.e., without any transparency function, and an intensity patch composed of arrays of pixels as shown in Fig. 4(b).

Therefore, stage of ensemble averaging is shifted from the rotating diffuser to the positional scanning of the spatially fluctuating random fields at the observation plane as highlighted by arrows in Figs. 4(a) & 4(b), 4(d) and 4(e).

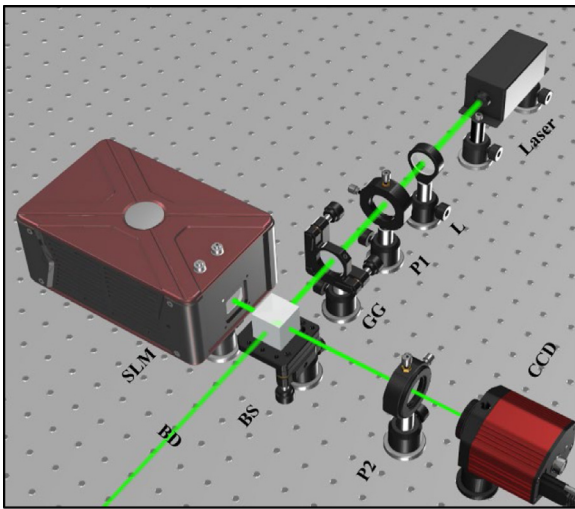


Fig. 3. Schematic of the experimental setup of the proposed technique, L: lens, P_n ($n = 1, 2$): Polarizers, GG: Ground glass, SLM: Spatial Light Modulator, BS: Beam splitter, CCD: Charge-Coupled device. BD-Beam Dumped.

4. Results and discussion

Taking a portion of the speckle pattern as a matrix $I_p(u_x, u_y)$ which represents one realization of the randomly scattered field as shown in Fig. 4. Here x and y are pixel spatial coordinates and may take values up to 300×300 pixels. For the field with transparency, we select only a central single pixel out of the 300×300 window, i.e., pixel (151,151) as shown in Figs. 4(a) and 4(d). The array of pixels 300×300 presents speckle without transparency as shown in Figs. 4(b) and 4(e). A small black square in the center of big red square represents only one pixel of the 300×300 window of object's random field in Figs. 4(a) and 4(d). This single pixel mimics the single pixel detector used in conventional GD schemes. The big red square in Figs. 4(b) and 4(e) represents the 300×300 window of random field without any object information. The single pixel of object speckle is correlated with the 300×300 pixels window of speckle without any object information. The red arrows represent that it is scanned over entire recorded speckle pattern of size 1000×1000 pixels. The cross-covariance of the intensity pattern is obtained by correlating $\Delta I_1(0,0)\Delta I_2(u_x, u_y)$ for different scanning positions as marked in Figs. 4(a), 4(b), 4(d) and 4(e), and the process of scanning is represented as $\sum_{m=1}^M (\Delta I_1^m(0,0)\Delta I_2^m(u_x, u_y)) / M$. Here M represents number of different windows of the matrix $I_p(u_x, u_y)$ and produced by the pixel-by-pixel movement of the matrix $I_p(u_x, u_y)$ over the speckle. We have used a speckle pattern of size 1000×1000 pixels and 2D scanning of $I_p(u_x, u_y)$ over the speckle patterns provide 700×700 different realizations. The spatial intensity correlation results for simulation and experiment for a transparency, i.e., an annular aperture (size 2.8 mm), are presented in Figs. 4(c) and 4(f) respectively. A random field is recorded at d and intensity correlation permits realization of a lensless Fourier transform even in the Fresnel domain. Simulation of the experimental situation is implemented under consideration of following steps: propagation of coherent light with transparency through a diffuser with random phase uniformly distributed between $[-\pi, \pi]$, use of the angular spectrum method for propagation. Subsequently, these simulated random intensities are used to evaluate cross-covariance of the intensities as defined in Eq. (13).

For simulation, we evaluate the Fourier pattern from the cross-correlation of intensity fluctuations as described earlier. A phase retrieval algorithm is applied to the far-field pattern to reconstruct the transparency.

Furthermore, recovery of two different transparencies, namely annular ring and sinusoidal grating from the intensity correlation is

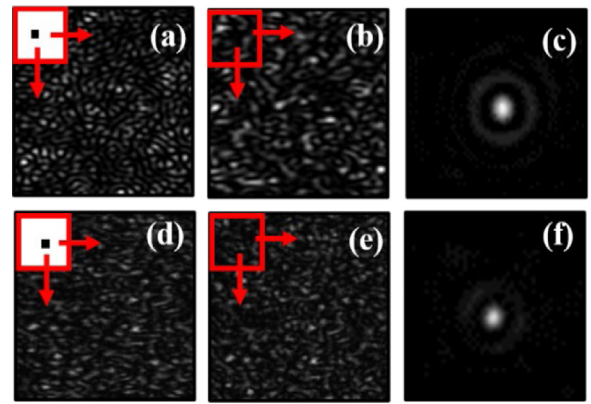


Fig. 4. Simulation Study (a-c): (a) only a single pixel of random field with transparency and scanning of single pixel in the space (b) window of the reference speckle and its scanning (c) Far-field pattern for annular aperture by simulation; Experimental Study (d-f): (d) only a single pixel of random field with transparency and scanning of single pixel in the space (e) window of the reference speckle and its scanning (f) Far-field pattern for annular aperture by experiment.

demonstrated. A phase retrieval algorithm (Fienup-type algorithm) is applied to the far-field pattern, using constraints that the $\tau(r)$ is real and positive. Moreover, we have also used a loose support constraint (the support is the set of points over which the object function is nonzero). Before applying the phase retrieval algorithm, a 2D Tucky window was used on the measured far field, to remove the noisy sections in intensity correlation function. A standard version of the phase retrieval algorithm is implemented in MATLAB software consisting of a hybrid input-output (HIO) algorithm with a fixed β value. An Error-Reduction algorithm is used to reduce the remaining noise from the retrieved image. For the quantitative analysis of the reconstructed results, we have calculated two parameters: visibility (v) and reconstruction efficiency (η) [33]. Visibility is defined as the extent to which the target reconstruction can be distinguished from the background noise and is measured as the proportion of the signal region's average intensity level to the background region's average intensity level in the reconstructed image. A global threshold technique is used to estimate the signal region. For annular ring, the calculated visibility values are 10.53 and 9.52 for simulation and experimental respectively. Similarly for second transparency i.e., sinusoidal grating, the visibility values for simulation and experiment are 8.70 and 8.46 respectively. Another important parameter for the quality evaluation is reconstruction efficiency (η), which is defined as the ratio of measured power in the signal region of the retrieved image to the sum of the measured powers in the signal and background regions. The efficiency values for annular ring are 0.91 and 0.89 respectively for simulation and experiment. The calculated η values for sinusoidal grating are 0.89 and 0.88 for simulation and experiment respectively.

Experimentally recorded random patterns for an annular ring are shown in Figs. 5(a) and 5(b). Fig. 5(a) shows a 1D pattern detected by a single pixel at different spatial points for a binary transmittance function 'ring'. A 2D reference random field without transparency is shown in Fig. 5(b). The original object i.e., annular ring transparency used for reconstruction is shown in 5(c). Reconstruction of the transparency from the intensity correlation of these two fields is shown in Fig. 5(d). Reconstruction of the 'ring' from the simulated random fields is also demonstrated and shown in Fig. 5(e).

We have also evaluated the reconstruction of a gradually changing transparency such as a sinusoidal function. The size of this transparency is restricted by an aperture of size 4.8 mm. Reconstruction of a sinusoidal grating transparency is shown in Fig. 6. Figs. 6(a) and 6(b) are 1D and 2D random fields. The original object i.e., sinusoidal grating transparency used for reconstruction is shown in 6(c) and

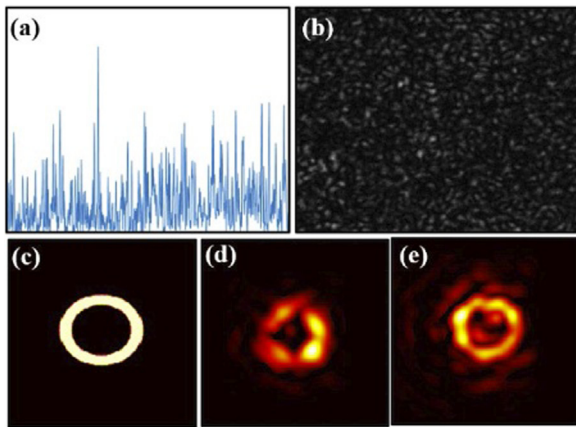


Fig. 5. (a) 1-D line profile for single-pixel used from object (Ring) experimental speckle (b) Experimentally recorded speckle without object information; (c) Original object; (d) and (e) indicate experimental and simulation reconstructed object transparency $\tau(r)$.

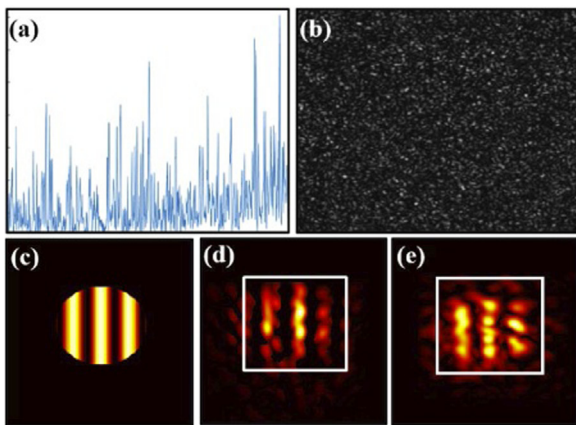


Fig. 6. (a) 1-D line profile for single-pixel used from Object (sinusoidal grating) (b) Experimentally recorded speckle without object information; (c) Original object; (d) and (e) indicate experimental and simulation reconstructed object transparency $\tau(r)$.

reconstruction of the transparency is shown in Figs. 6(d) and 6(e) for experimental and simulated cases respectively.

The slight variation in experiment and simulation results arises due to experimental limitations such as limited size optics, and limited size of recorded speckle patterns. The reconstruction quality further depends on the factors like correlation length of the source, i.e., illumination speckle size at the object plane, and also the number of speckle grains (independent patches) available at the recording plane for spatial averaging. Quality of retrieved results is effectively determined by the size of the Tuckey window used in the phase retrieval algorithm. A 2D Tuckey window is applied to the correlation function of intensity fluctuations in order to avoid the noisy region of the correlation. The higher frequency content of the intensity Fourier spectrum is influenced by the size of the Tukey window used to filter the speckle autocorrelation function, and as a result, affects the object reconstruction.

5. Conclusion

In conclusion, we have proposed and experimentally demonstrated a new ghost diffraction scheme by exploiting the correlation features of the spatially varying random fields. Based on the new strategy, the technique is capable of reconstructing the object by utilizing the spatial points in the random pattern. The novelty of the technique lies in the significant use of spatial averaging over temporal averaging as used in conventional ghost diffraction scheme. This leads to reconstruct

the transparency with only two-time frozen random patterns. The simulation and experimental results are presented for two different objects. The technique opens a wide range of applications in microscopy, imaging and encryption.

Funding

This work is supported by Science and Engineering Research Board (SERB) India- CORE/2019/000026 and Council of Scientific and Industrial Research (CSIR), India- Grant No 80 (0092)/20/EMR-II.

Declaration of competing interest

The authors declare that they have no known competing financial interests or personal relationships that could have appeared to influence the work reported in this paper.

Data availability

Data will be made available on request.

Acknowledgments

Manisha acknowledges fellowship from the IIT (BHU). Vipin Tiwari would like to acknowledge support from DST-INSPIRE (IF-170861).

Declaration of competing interest

The authors declare that they have no known competing financial interests or personal relationships that could have appeared to influence the work reported in this paper.

References

- [1] R.H. Brown, R.Q. Twiss, Correlations between photons in two coherent beam of light, *Nature* 177 (1956) 27–32, <http://dx.doi.org/10.1038/177027a0>.
- [2] J. Rosen, V. Anand, M.R. Rai, S. Mukherjee, A. Bulbul, 3D imaging by coded aperture correlation holography (COACH), *Appl. Sci. Rev.* 9 (2019) 605, <http://dx.doi.org/10.3390/app9030605>.
- [3] A. Gatti, E. Brambilla, M. Bache, L.A. Lugiato, Correlated imaging, quantum and classical, *Phys. Rev. A* 70 (2014) 013802, <http://dx.doi.org/10.1103/PhysRevA.70.013802>.
- [4] M.J. Padgett, R.W. Boyd, An introduction to ghost imaging: quantum and classical, *Philos. Trans. R. Soc. A* 375 (2017) 20160233, <http://dx.doi.org/10.1098/rsta.2016.0233>.
- [5] P.A. Moreau, E. Toninelli, T. Gregory, M.J. Padgett, Ghost imaging using optical correlations, *Laser Photonics Rev.* 12 (2018) 1700143, <http://dx.doi.org/10.1002/lpor.201700143>.
- [6] J.H. Shapiro, R.W. Boyd, The physics of ghost imaging, *Quantum Inf. Process.* 11 (2012) 949–993, <http://dx.doi.org/10.1007/s11128-011-0356-5>.
- [7] C. Zhao, W. Gong, M. Chen, E. Li, H. Wang, W. Xu, S. Han, Ghost imaging lidar via sparsity constraint, *Appl. Phys. Lett.* 101 (2012) 141123, <http://dx.doi.org/10.1063/1.4757874>.
- [8] M. Padgett, R. Aspden, G. Gibson, M. Edgar, G. Spalding, Ghost imaging, *Opt. Photonics News* 27 (2016) 38–45, <http://dx.doi.org/10.1364/OPN.27.10.000038>.
- [9] T.B. Pittman, Y.H. Shih, D.V. Strekalov, A.V. Sergienko, Optical imaging by means of two-photon quantum entanglement, *Phys. Rev. A* 52 (1995) R3429, <http://dx.doi.org/10.1103/PhysRevA.52.R3429>.
- [10] D.V. Strekalov, A.V. Sergienko, D.N. Klyshko, Y.H. Shih, Observation of two-photon ghost interference and diffraction, *Phys. Rev. Lett.* 74 (1995) 3600, <http://dx.doi.org/10.1103/PhysRevLett.74.3600>.
- [11] R.S. Bennink, S.J. Bentley, R.W. Boyd, Two-photon coincidence imaging with a classical source, *Phys. Rev. Lett.* 89 (2002) 113601, <http://dx.doi.org/10.1103/PhysRevLett.89.113601>.
- [12] A. Gatti, E. Brambilla, M. Bache, L.A. Lugiato, Ghost imaging with thermal light: Comparing entanglement and ClassicalCorrelation, *Phys. Rev. Lett.* 93 (2004) 093602, <http://dx.doi.org/10.1103/PhysRevLett.93.093602>.
- [13] F. Ferri, D. Magatti, A. Gatti, M. Bache, E. Brambilla, L.A. Lugiato, High-resolution ghost image and ghost diffraction experiments with thermal light, *Phys. Rev. Lett.* 94 (2005) 183602, <http://dx.doi.org/10.1103/PhysRevLett.94.183602>.

- [14] N.D. Hardy, J.H. Shapiro, Reflective ghost imaging through turbulence, *Phys. Rev. A* 84 (2011) 063824, <http://dx.doi.org/10.1103/PhysRevA.84.063824>.
- [15] T. Shirai, T. Setälä, A.T. Friberg, Temporal ghost imaging with classical non-stationary pulsed light, *J. Opt. Soc. Amer. B* 27 (2010) 2549–2555, <http://dx.doi.org/10.1364/JOSAB.27.002549>.
- [16] Z. Sun, F. Tuijete, C. Spielmann, Toward high contrast and high-resolution microscopic ghost imaging, *Opt. Express* 27 (2019) 33652–33661, <http://dx.doi.org/10.1364/OE.27.033652>.
- [17] D. Faccio, Temporal ghost imaging, *Nat. Photonics* 10 (2016) 150–152, <http://dx.doi.org/10.1038/nphoton.2016.30>.
- [18] P. Zerom, Z. Shi, M.N. O'Sullivan, K.W.C. Chan, M. Krogstad, J.H. Shapiro, R.W. Boyd, Thermal ghost imaging with averaged speckle patterns, *Phys. Rev. A* 86 (2012) 063817, <http://dx.doi.org/10.1103/PhysRevA.86.063817>.
- [19] J.H. Shapiro, Computational ghost imaging, *Phys. Rev. A* 78 (2008) 061802, <http://dx.doi.org/10.1103/PhysRevA.78.061802>.
- [20] Z. Zhang, X. Wang, G. Zheng, J. Zhong, Hadamard single-pixel imaging versus Fourier single-pixel imaging, *Opt. Express* 25 (2017) 19619, <http://dx.doi.org/10.1364/OE.25.019619>.
- [21] X. Nie, X. Zhao, T. Peng, M.O. Scully, Sub-Nyquist computational ghost imaging with orthonormal spectrum-encoded speckle patterns, *Phys. Rev. A* 105 (2022) 043525, <http://dx.doi.org/10.1103/PhysRevA.105.043525>.
- [22] D. Zhang, Y.-H. Zhai, L.-A. Wu, X.-H. Chen, Correlated two-photon imaging with true thermal light, *Opt. Lett.* 30 (2005) 2354–2356, <http://dx.doi.org/10.1364/OL.30.002354>.
- [23] A. Valencia, G. Scarcelli, M. D'Angelo, Y. Shih, Two-photon imaging with thermal light, *Phys. Rev. Lett.* 94 (2005) 063601, <http://dx.doi.org/10.1103/PhysRevLett.94.063601>.
- [24] R. Borghi, F. Gori, M. Santarsiero, Phase and amplitude retrieval in ghost diffraction from field-correlation measurements, *Phys. Rev. Lett.* 96 (2006) 183901, <http://dx.doi.org/10.1103/PhysRevLett.96.183901>.
- [25] P. Clemente, V. Durán, E. Tajahuerce, V. Torres-Company, J. Lancis, Single-pixel digital ghost holography, *Phys. Rev. A* 86 (2012) 041803, <http://dx.doi.org/10.1103/PhysRevA.86.041803>.
- [26] T. Shirai, T. Setälä, A.T. Friberg, Ghost imaging of phase objects with classical incoherent light, *Phys. Rev. A* 84 (2011) 041801, <http://dx.doi.org/10.1103/PhysRevA.84.041801>.
- [27] D.J. Zhang, Q. Tang, T.F. Wu, H.C. Qiu, D.Q. Xu, H.G. Li, H.B. Wang, J. Xiong, K. Wang, Lensless ghost imaging of a phase object with pseudo-thermal light, *Appl. Phys. Lett.* 104 (2014) 121113, <http://dx.doi.org/10.1063/1.4869959>.
- [28] R.V. Vinu, Z. Chen, R.K. Singh, J. Pu, Ghost diffraction holographic microscopy, *Optica* 7 (2020) 1697–1704, <http://dx.doi.org/10.1364/OPTICA.409886>.
- [29] M. Takeda, W. Wang, D.N. Naik, R.K. Singh, Spatial statistical optics and spatial correlation holography: A review, *Opt. Rev.* 21 (2014) 849–861, <http://dx.doi.org/10.1007/s10043-014-0138-2>.
- [30] J.R. Fienup, Reconstruction of an object from the modulus of its Fourier transform, *Opt. Lett.* 3 (1978) 27–29, <http://dx.doi.org/10.1364/OL.3.000027>.
- [31] J.R. Fienup, Phase retrieval algorithms: a comparison, *Appl. Opt.* 21 (1982) 2758–2769, <http://dx.doi.org/10.1364/AO.21.002758>.
- [32] B. Das, N.S. Bisht, R.V. Vinu, R.K. Singh, Lensless complex amplitude image retrieval through a visually opaque scattering medium, *Appl. Opt.* 56 (2017) 4591–4597, <http://dx.doi.org/10.1364/AO.56.004591>.
- [33] T.R. Hillman, T. Yamauchi, W. Choi, R.R. Dasari, M.S. Feld, Y. Park, Z. Yaqoob, Digital optical phase conjugation for delivering two-dimensional images through turbid media, *Sci. Rep.* 3 (2013) 1–5, <http://dx.doi.org/10.1038/srep01909>.